

any further increase in activation controlled processes. As would be expected, however, this condition is delayed if the bulk-dissolved oxygen content is increased or if the solution flow rate is increased; both of these actions effectively increase the concentration of oxygen and reduction kinetics at the reacting metal surface. This is illustrated in Figure A.6 by the vertical lines marked i_l 1, 2, 3, 4, 5, and 6. It is apparent that the corrosion current density and corrosion potential can change in a non-monotonic manner with different changing system conditions (e.g., flow rate, oxidant concentration, turbulence), but these can be predicted via knowledge of the oxidation rates and the reduction rates associated, in this example, with dissolved oxygen content, solution flow rate, etc.

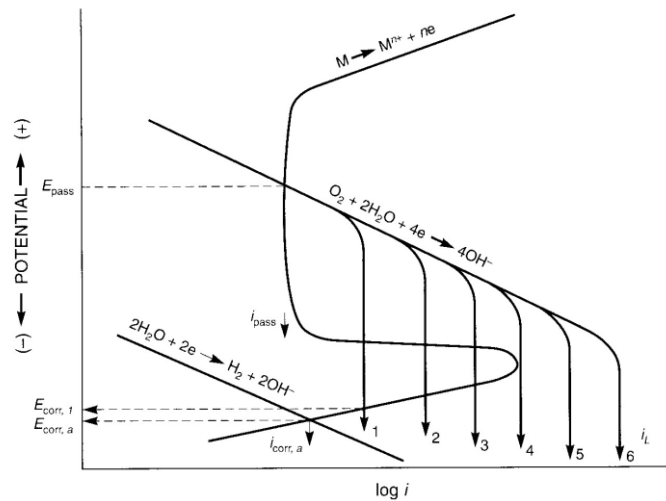


Fig. A.6 Superposition of the reduction kinetics for dissolved oxygen on the metal oxidation rates from Figure A.5. In this case the reduction kinetics may be limited by the supply of oxygen to the reacting surface. [4] (Reprinted by Permission of Pearson Education, Inc., Upper Saddle River, NJ.)

A.4 Description of Degradation Modes and their Predictability in LWRs

A.4.1 “Uniform” Corrosion

This section addresses degradation mechanisms, which result in loss of material over a reasonably large area (as opposed to localized corrosion that may occur over areas governed by metallurgical inhomogeneity defined broadly as less than 1-2 cm²). Such “uniform” degradation modes include general corrosion, boric acid corrosion and flow accelerated corrosion.

General Corrosion

General corrosion is characterized by uniform surface loss through material oxidation (i.e., general Equations A.1-A.3), and is deleterious to plant operation due to (a) loss of functionality of a pressure boundary due to loss of section thickness, (b) the presence of corrosion products (“crud”) which may decrease the heat transfer efficiency when these deposit on e.g., steam generator tubes or fuel cladding, and (c) the presence of crud which is deposited and activated on the fuel cladding surface and, upon release, will increase the radioactivity levels in the RCS or, in the case of direct cycle BWRs, the balance of plant.

General corrosion issues are part of the design basis of the LWRs and are founded on a large body of research over many decades. Thus there is good reason for the judgments in Table A.5 that general corrosion is usually not an issue in LWRs. The following discussion is included, however, since the electrochemical details of general corrosion in LWRs forms a basis for understanding other corrosion-based degradation modes for which there may be less confidence in our ability to adequately address the situation.

As explained in Section A.3 the corrosion rates may be managed by consideration of the thermodynamically stable (or metastable) species (dissolved metal cations, oxides, salts, etc.) at the metal/water interface and the control of the relevant oxidation and reduction kinetics. In the case of the main materials of construction in LWRs importance is attached to the surface oxide solubility, which, as indicated in Figure A.7, for magnetite in the iron/water system at 300°C, exhibits a minimum at neutral or slightly alkaline conditions [9]. Very similar solubility /pH relationships are noted for chromium and nickel. Also shown in Figure A.7 is the dependency of the corrosion rate for mild steel on pH, which mirrors the oxide solubility dependency.

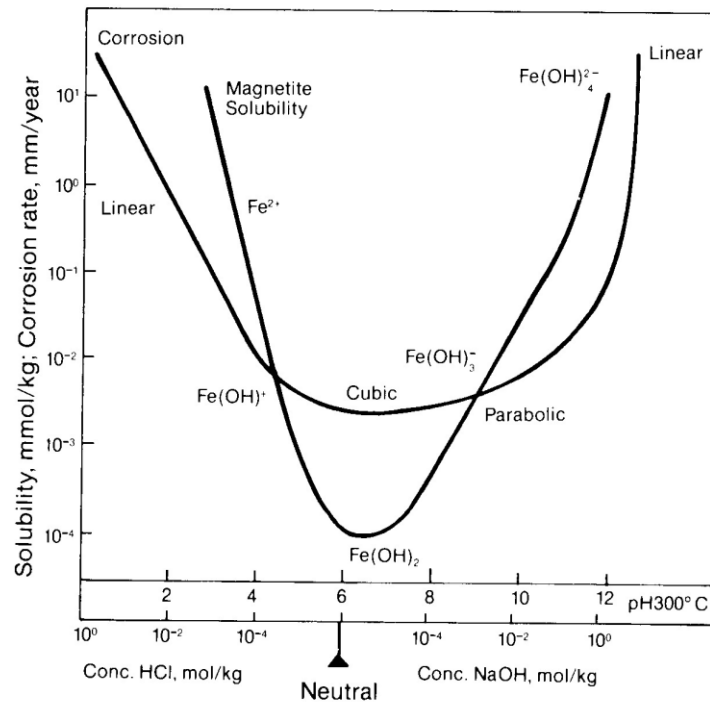


Fig. A.7 Corrosion of mild steel and solubility of magnetite at 300°C showing corrosion rate laws [9]

As explained in Section A.3 the corrosion rates of stainless steels and nickel-base alloys in high temperature water are significantly lower than those of carbon steels due to spinel type oxides composed of a mixture of NiFe₂O₄, Fe₃O₄ and FeCr₂O₄. Consequently in the high temperature RCS, the internal surfaces of the low alloy steel pressure vessel, pressurizer and steam generator are clad with type 308/309 stainless steels. However there are carbon steel components exposed to high temperature water/wet steam such as feedwater piping, main steam lines and some parts of the pressure vessel left exposed following repair procedures at, for instance, vessel penetrations such as CRDM or instrumentation tubes. For these reasons, amongst others

associated with control of localized corrosion, both PWR and BWR operations are subject to strict water chemistry control, as discussed below.

Because of the dependencies of corrosion rate and oxide solubility on pH, the water chemistry specifications for PWRs impose a tight control on the pH values, which may vary slightly from one plant to another, and between primary [see Appendix B.11] and secondary [see Appendix B.12] systems. This control is achieved via injection from the Chemical Volume and Control System (CVCS) to the primary system of LiOH, and boric acid (for chemical shim control of core reactivity). Early water chemistry specifications imposed a $\text{pH}_{300\text{C}}$ specification of 6.9 ± 0.2 , corresponding to the minimum in magnetite solubility (Figure A.7), but more recent specifications have increased this $\text{pH}_{300\text{C}}$ specification range to 7.1-7.3, in order to take advantage of both the corrosion resistance due to nickel ferrite and the improved control of crud build up and shutdown dose rates. There is a limit to which this alkalinity increase can be allowed which is associated with an increase both in corrosion rate of zirconium alloy fuel cladding, and in susceptibility to stress corrosion cracking of Alloy 600 steam generator tubing.

In addition to pH control for PWRs associated with the thermodynamic stability of a protective oxide on the surface, the kinetics of corrosion are also, as discussed in section A.3, a function of the presence of oxidizing species. Consequently, the RCS primary system has an overpressure (approx. 15 KPa) of hydrogen to minimize the reduction kinetics of Equation A.7. A maximum limit in the amount of hydrogen overpressure is determined by avoidance of hydriding of the zirconium alloy cladding. Additional overpressure via operation of the pressurizer also ensures that, under normal operating conditions, boiling in the reactor core is largely suppressed, thereby minimizing the possibility of concentration of, e.g., impurities at heat transfer surfaces in the primary side and the consequent increase in corrosion rate at these boiling sites.

In the PWR secondary system the dissolved oxygen concentration (which affects both the activation and diffusion controlled reduction kinetics and, thereby, the metal corrosion rate), is controlled by the presence of hydrazine [see Appendix B.12]. However since boiling occurs on the secondary side of the steam generator tubes, it is possible to have accelerated corrosion in occluded regions such as tube/tube support regions; this will be discussed later in the section on crevice corrosion.

Control of general corrosion in the lower temperature systems such as the service water system, where the piping is predominately carbon steel, can present a potential problem since the water supplies for such systems are “uncontrolled” sources such as the ultimate heat sink, lake water, or sea water. Moreover, under such lower temperature conditions the surface oxide is not as protective as that at higher temperatures in the pH range specified for, e.g., the RCS. However, generally accepted corrosion prevention methods widely used in other industries (transportation, petrochemical, marine, etc.) are applied, including the use of cathodic protection, (for submerged pumps and underground piping), inhibitors (such as phosphates) or biocides to control microbiologically induced corrosion.

Chemistry control for general corrosion in direct cycle BWRs is largely driven by the fact that, under “normal water chemistry” (NWC) conditions, there is an excess of dissolved oxygen in the coolant, since the other product of the radiolytic breakdown of water, hydrogen, is preferentially partitioned to the steam phase. This dissolved oxygen has a deleterious effect on stress corrosion cracking of most of the BWR materials of construction, as will be discussed later. Consequently the main driving force in chemistry control for BWRs [see Appendix B.10] has been to lower the dissolved oxygen concentration (or more accurately, the corrosion potential) by both injection of hydrogen (**Hydrogen Water Chemistry**) and control of the dissolved impurity level.

As a result of these industry actions, the level of impurity contents in the reactor coolant has dropped markedly over the last few decades, with current coolant conductivities approaching that of theoretically pure water; moreover, virtually all of the U.S. BWRs now operate under HWC with modifications due to the addition of noble metals (Noblechem™) to the coolant that improve the efficiency of the oxygen/hydrogen recombination [10, 11, see Appendix B.10].

Although these actions have been extremely effective in controlling stress corrosion, the addition of hydrogen can have a deleterious impact on radioactivity release due to both ^{16}N during power operation and the creation and release of activated corrosion byproducts, mainly ^{60}Co , during plant shutdown and/or changes between NWC and HWC.

In the former case the release of ^{16}N to the steam and off-gas systems is aggravated by the addition of hydrogen to the coolant and the effect that this has on the formation of volatile nitrogen bearing species originating from $^{16}\text{O}(n,p)^{16}\text{N}$ reactions in the core region. This increase in the ^{16}N content effectively limits the hydrogen addition to the feedwater to 200-300 ppb. In more recent times the widespread adoption of noble metal technology, and especially Noblechem™, has minimized the HWC/ ^{16}N problem and has allowed the efficient reduction of the corrosion potential without the deleterious radioactivity offgas release [11].

The creation and release of ^{60}Co is directly relatable to the presence of ^{59}Co in corrosion products from cobalt-rich, wear resistant Stellite valve seatings, roller bearings, etc, or to cobalt impurities in the nickel base components and stainless steel piping and, especially, control rod blade sheaving. Once this crud is deposited and the ^{59}Co is activated on the fuel cladding, the resultant ^{60}Co is transported to the stainless steel piping where it is incorporated into the oxide spinel structure. The mitigation for this deleterious general corrosion related phenomenon [see Appendix B.10] is to (a) reduce the cobalt inventory in the reactor circuit by using alternatives to cobalt-rich Stellites, (b) minimizing the crud formation (which acts as a transport vehicle for the activated ^{60}Co from the core to the piping) by control of the anionic impurity and the dissolved iron concentrations and, (c) add 10-100ppb zinc to the coolant. In this latter case the zinc inhibits the corrosion of stainless steel, resulting in thinner spinel films, and also takes up competing sites where ^{60}Co could reside in the oxide spinel structure.

Although the reduction in dissolved oxygen content and corrosion content via HWC/ Noblechem™ has been successful in reducing the extent of stress corrosion cracking in BWRs, it has introduced a problem of increased corrosion of carbon steel feedwater lines [12,13] due to the formation of non-protective magnetite films at the low corrosion potentials associated with oxygen contents <5-10 ppb. Consequently BWR water chemistry guidelines [see Appendix B.10] specify a minimum dissolved oxygen content of 30 ppb in the feedwater lines to ensure the creation of a more adherent and protective magnetite film which is stable at the more elevated corrosion potentials.

From a life-management standpoint, it is apparent that the knowledge base exists to predict and control the general corrosion behavior in most of the materials of construction in LWRs via appropriate water chemistry control. Indeed there is some considerable margin in the design basis to account for general corrosion since actual corrosion rates are significantly below the design-basis allowable values. For instance, the design specification provides a general corrosion allowance of 120 mils for the carbon steel main steam system. The actual general corrosion rate for carbon steel piping in a steam environment is less than 0.16 mils per year. Similarly, the corrosion allowance for stainless steel piping operating in the 260-316EC (500-600°F) range is 2.4

mils. The actual general corrosion rate for stainless steel in this temperature range is 0.01 mils/year of service life.

Boric Acid Corrosion

Although, as discussed in the section above, the general corrosion rates of the LWR materials of construction are well below the design values required to maintain structural integrity, and the radioactivity issues associated with activation of the corrosion products can be managed, there are situations where very high corrosion rates can occur over significant areas.

One such situation is the corrosion of carbon and low alloy steels due to boric acid in PWR primary environments [14, 15, see Appendix B.18,]. Under normal operating conditions the corrosion rate of carbon and low alloy steels in borated, hydrogenated, primary water is <0.025 mm/year, but problems have occurred in operating plants when borated water leaks from the PWR RCS onto an external carbon or low alloy steel surface. Under these leakage situations the boric acid concentration on the external component will increase due, for instance, to steam flashing and alternate wetting and drying cycles that produce, ultimately, a low pH boric acid slurry which, in combination with an oxygenated air atmosphere, can cause very high corrosion rates of approximately 25 mm/year, (Figure A.8). Such an increase in corrosion susceptibility is predictable via reference to the Pourbaix diagram for the iron/water system (Figure A.1), which indicates that, under acidic, and especially under higher surface potential, oxygenated conditions, corrosion is likely, and that it is unlikely that any protection due to a surface oxide would be forthcoming given the high oxide solubility under these acidic conditions (Figure A.7).

Problems of boric acid wastage of closure studs in the pressurizer, reactor coolant pump, steam generator manways, etc. have been associated with leaks due to gasket failures or through wall cracks in the component. The most notable recent observation of such a degradation mode was the through-wall corrosion of the pressure vessel head at Davis Besse in 2002 associated with stress corrosion cracking of nickel-base alloys in the vessel head penetration assembly and subsequent leakage of primary coolant into a restricted geometry between the outside of the pipe and the reactor pressure vessel head. The result was that boric acid concentrated due to boiling and evaporation to levels that led to excessive corrosion of the low alloy steel pressure vessel. All of these incidents are in the higher temperature RCS where such concentration mechanisms are possible. By contrast, boric acid wastage problems would not be expected to be associated with leaks in lower temperature systems (<100°C) such as the ECCS and CVCS since, although these systems are borated, there would be no mechanism to concentrate the boric acid sufficiently to achieve the low pH values needed for high low alloy steel corrosion rates.

As indicated in Figure A.8 the corrosion rate of carbon and low alloy steels increases with increasing acidity and is, depending on the pH value greatest at temperatures between 80 and 150°C. Such a surface temperature range is achievable due to evaporative cooling of the escaping high pressure coolant impacting on the external component.

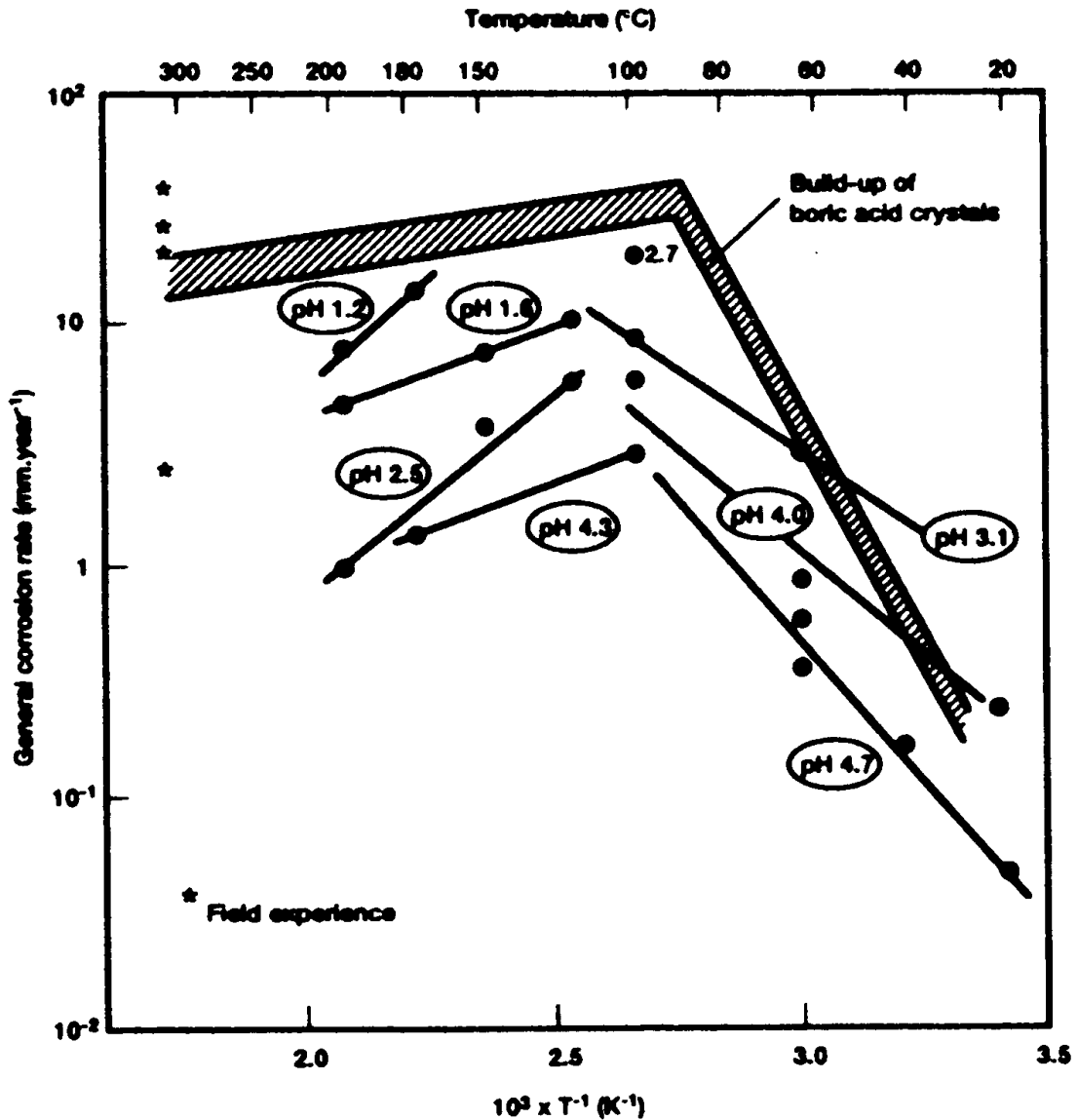


Fig. A.8. Relationship between the corrosion rate of carbon and low alloy steels in various acidified boric acid solutions as a function of temperature. [15]

As discussed in Appendix B.18, the Davis Besse incident does present some challenges to the assertion that all boric acid wastage is predictable since, in this particular geometry, it was unclear that very low pH values could be achieved. As a result there are ongoing research efforts both in the industry and the NRC to determine, for instance, the interactions between the corrosion rate and various factors such as the leakage rate (and the role of erosion –corrosion or impingement), the chemistry of the escaping coolant, the extent of evaporative cooling of the low alloy steel surface, and the role of the geometry of the assembly (for instance, the dimensions of the annulus between the CRDM pipe and the pressure vessel in the case of Davis Besse), which will affect the mass transport of oxygen and liquid within the crevice.

Flow-Accelerated Corrosion and Erosion-Corrosion

Flow-accelerated corrosion is frequently localized at areas of high turbulence, often associated with geometrical discontinuities or abrupt changes in flow direction, and this manifests itself as a localized wall loss. There are well-defined electrochemical and mechanical reasons for such degradation since the water or steam flow past the metal component may increase the kinetics of corrosion in various ways, as discussed below.

At the simplest level the corrosion kinetics may be increased under both laminar and turbulent flow regimes due to an increase in diffusion rates of, for instance, dissolved oxygen, to the metal surface, or the increase in removal rate of oxidized species from the metal surface. These concepts were discussed in relation to Figure A.6. If the oxide film has a two layer structure, as seen and discussed above for the general corrosion of carbon and low alloy steels in high temperature water, (Figure A.9), then increasing flow rate may also remove the outer oxide layer under turbulent flow conditions. Under these conditions the flow-accelerated corrosion rates will be controlled ultimately by the reductive dissolution of the inner oxide layer and the diffusion kinetics of Fe(II) species away from the surface. Under such conditions the corrosion rate may be considerably enhanced and be of the order of 10 mm/year.

It is apparent that these controlling conditions are primarily electrochemical in nature. It is also possible to accelerate the corrosion rate even further by imposing a mechanical factor to the removal of the outer oxide layer, including the effect of the impact of water droplets on the surface in two phase flow steam systems (e.g., wet steam in main steam lines or cross-around piping in turbines), cavitation effects (e.g., impeller blades in pumps) or, in extreme situations, entrained particles, such as sand, in service water systems. Such mechanically dominated effects are normally described as “erosion-corrosion” or “erosion” depending on the degree of the mechanical contribution.

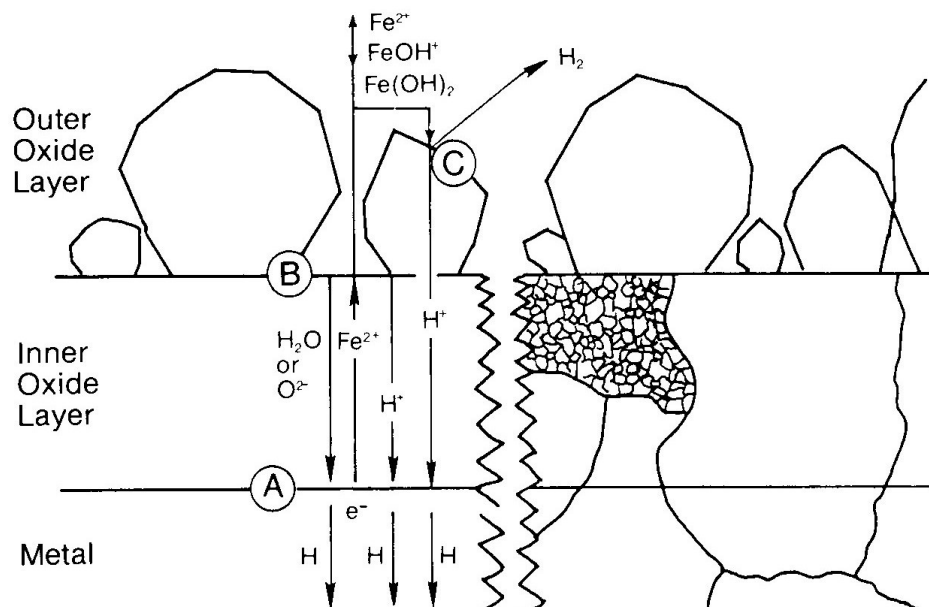


Fig. A.9. Schematic of two-layer oxide structure on carbon steel in high temperature water. [16] (© NACE International 1981)

As mentioned above, the extent of flow-accelerated electrochemically-controlled corrosion in high temperature aqueous environments is very much a function of the material/environment combinations that affect the structure of the oxide layers and their chemical and mechanical stability. Following the catastrophic failure of a carbon steel suction line to the main feedwater pump at Surry-2 PWR [17], there was considerable study [18] of the factors controlling flow accelerated corrosion in LWRs, leading up to the development by EPRI of the CHECWORKS™ prediction code [19]. As discussed in more detail in Appendix B.17, the flow rate effect on the corrosion rate for carbon or low alloy steels is a function of the material composition, piping geometry, single vs. two-phase environment, temperature, pH, laminar vs. turbulent flow and the local corrosion potential. As indicated in Figure A.10 for flow accelerated corrosion of carbon steel in deoxygenated ammoniated water, the corrosion rate is a non-monotonic function of temperature, with a maximum occurring in the range of 130-150°C for single phase fluids; the peak corrosion rates occur at a higher temperature range for two-phase environments (e.g., wet steam in the main steam line and turbine cross-around piping).

Control of the local corrosion potential (or dissolved oxygen content) is a key factor in managing flow accelerated corrosion of carbon and low alloy steels in the main steam, feedwater, condensate and moisture separator piping in BWRs. As indicated in Figure A.11, the flow-accelerated corrosion rates in condensate and moisture separator reheater drain systems are a function of the local dissolved oxygen content; such an observed relationship is in agreement with the CHECWORKS™ predictions.

The ability to minimize the corrosion rate by maintaining the local dissolved oxygen content above 30 ppb will be a function of the amount of air in-leakage from the turbine condenser and, as mentioned earlier in the general corrosion section, the degree of oxygen dosing in the feedwater lines. The amount of oxygen control required to minimize flow-accelerated corrosion in the two-phase environment in the main steam line will be a function of the amount of radiolysis occurring in the reactor core, the degree of hydrogen water chemistry/ Noblechem™ and the extent of venting being applied in the moisture separators. The ultimate remedy is to make use of the more protective and adherent films associated with chromium alloying; hence the replacement of the susceptible lines with low alloy steels with higher chromium content, stainless steels or the use of a higher chromium content coating deposited by thermal spray or weld overlay.

The message here is that the extent of flow-accelerated corrosion that can occur in carbon and low alloy steels in PWRs and BWRs is predictable, and the mechanism is understood. The prediction algorithms (i.e., CHECWORKS™) are routinely used in individual plant Aging Management Programs to assign inspection priorities. It has generally been found that, where problems do occur, it is apparent that these analyses and inspection priority methodologies have not been followed.

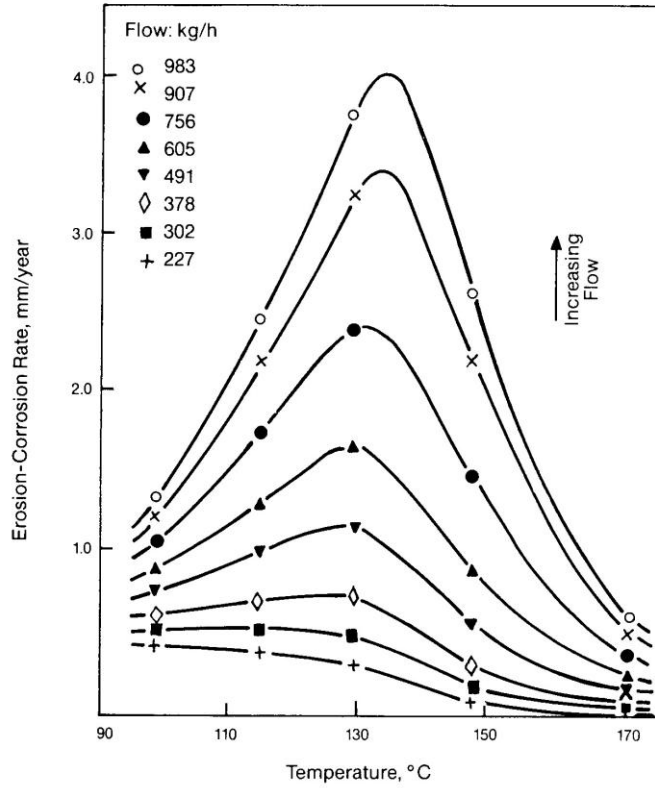


Fig. A.10. Effect of temperature on the flow accelerated corrosion rate of carbon steel in deoxygenated ammoniated water. [20] (DR 1982 EDF)

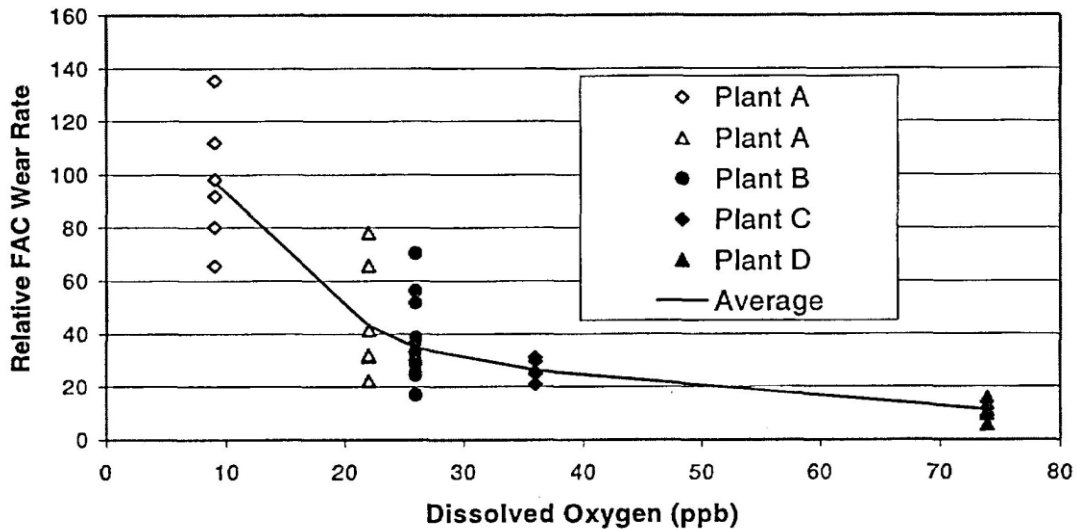


Fig. A.11. Flow-accelerated corrosion data for condensate and moisturizer separator re-heater drain systems in four BWR plants as a function of the local dissolved oxygen contents [Appendix B.10]

A.4.2 Localized Corrosion

This section addresses materials degradation modes, where the corrosion damage occurs over relatively small areas but, potentially, may occur at high penetration rates. The result in such cases may be localized leakage or, in more extreme situations, lack of structural integrity and catastrophic failure. Such degradation modes include, crevice, pitting, galvanic and microbially induced corrosion and environmentally assisted cracking. This latter category includes stress corrosion cracking, strain-induced cracking, and corrosion fatigue (discussed in Section A.4.4 on Fatigue).

Crevice Corrosion

As the title suggests, this phenomenon is associated with crevices inside which a relatively stagnant solution is present and where there is a mechanism to make that solution more aggressive (e.g., increased acidity and increased anionic impurity concentration), and thereby increase the local metal corrosion rate. The crevices may be inherent in the component design (such as at gaskets, lap joints, bolt heads and threads), or may occur under corrosion deposits and sludge piles. The critical factors in controlling this form of attack are (a) the geometry of the crevice, and the conditions that affect the thermal hydraulics within the crevice, and (b) the mechanisms that change the cationic and anionic concentrations within the crevice.

The thermal hydraulics and mechanisms of crevice corrosion have been extensively researched over the last 30 years and, as a result, control techniques are available (see, for instance, References 21 and 22). Examples of this understanding/control synergy are given below.

As indicated schematically in Figure A.12 there is the possibility that, in aerated solutions, the site for oxygen reduction is concentrated on the exposed surface at the mouth of the crevice. A reason for this is that the convection-controlled transport rate of dissolved oxygen into the crevice is insufficient to make up for the removal of dissolved oxygen due to general corrosion on the crevice sides. The resultant separation of the oxygen reduction site at the crevice mouth from the metal oxidation site at the tip of the crevice imposes a potential gradient down the crevice, thereby giving rise to potential-driven diffusion of anionic impurities (e.g., chloride) to the crevice tip. In order to maintain electroneutrality it is necessary that there be an increase in acidity within the crevice by, for instance, the hydrolysis of the dissolved metal cations (Equation A.4). Thus, the environmental conditions of low pH and high anionic impurity concentration are created within the crevice that could lead to an increase in metal corrosion rate.

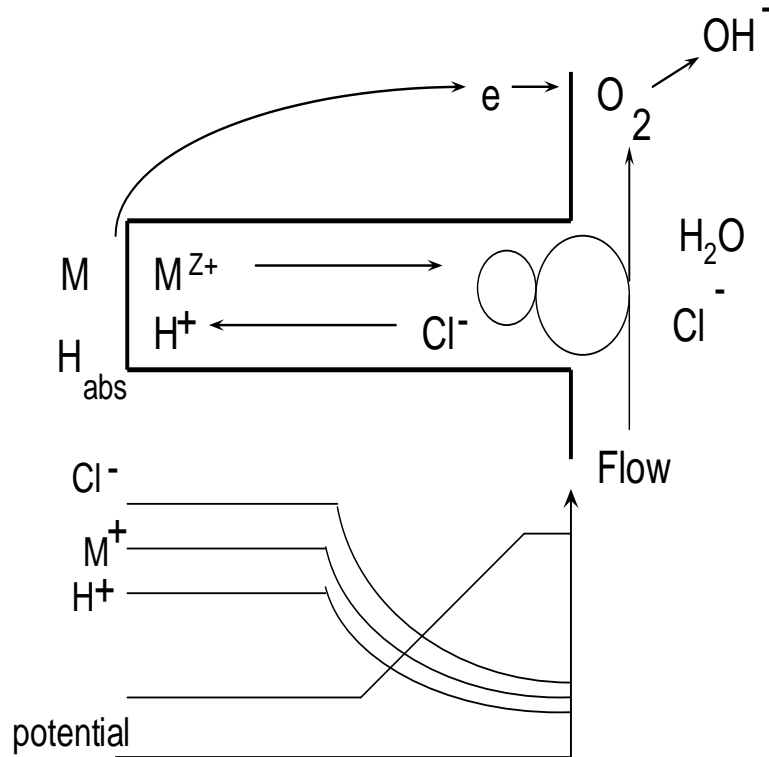


Fig. A.12. Schematic of crevice in aerated solution, indicating the separation of the metal oxidation and oxygen reduction sites, and the consequent changes in pH and anionic concentrations

A further crevice corrosion mechanism is possible at heat transfer surfaces, where concentrations of species may occur due to their distribution between the aqueous and gaseous (e.g., steam) phases or the evaporation of volatile species. This concentration of acidity, alkalinity, or other aggressive non-OH⁻ anions may be retained in an occluded region under specific geometrical conditions which inhibit solution redistribution. A classical example of this is the localized corrosion of carbon steel tube support plates in PWR steam generators, as illustrated in Figure A.13 [see Appendix B.7], which has led to denting of the Alloy 600 tube and subsequent stress corrosion cracking on the primary and secondary sides of the tube.

Pitting Corrosion

Pitting corrosion has very similar attributes to crevice corrosion in that it depends in part on the creation of a localized environment; however the important difference is that the geometric features that lead to degradation are inherent in the material microstructure and may be manifested by long incubation periods before the pits grow. Again this is a topic that has received much attention and research [8, 21, 22, 24, 25] over many decades and is covered in part in Appendix B.3. Thus the judgment indicated, for instance, in Table A5 is that there is adequate understanding to manage this phenomenon in LWRs, with the biggest uncertainty being associated with reactor systems where there might be lesser knowledge or control over the environmental conditions.

Quantitative models for predicting and controlling pitting corrosion in nuclear systems focus on taking into account the following sequence of events:

(a) Localized breakdown of the surface oxide, usually due to the presence of aggressive anions. The aggressive anions are normally associated with chlorides originating from, for example, condenser leaks, but damage can also be associated with other halides, or with sulfates, perchlorates, etc. The metallurgical sites for such oxide breakdown may be random, but are usually associated with inhomogeneities such as surface breaking precipitates or with grain boundaries over which the oxide is of a less protective nature. The breakdown of the oxide occurs at surface potentials above a critical value (known as the “pitting potential”), which is a function of the anion type and its concentration, the material composition, temperature, etc. Thus pitting is a possible concern if the corrosion potential is more positive than the pitting potential, and such a criterion puts a limitation on the system conditions under which pitting corrosion would be a problem. This is illustrated in Figure A.14 by the temperature dependence of the corrosion potential and pitting potential of Alloy 600 in water containing various concentrations of chloride. [26, 27] It is seen that under low dissolved oxygen conditions the corrosion potential is always lower than the pitting potential (for the indicated range of chloride concentrations) and, therefore, over a wide temperature range, pitting should not be a concern. At higher oxygen content conditions, however, pitting might be a concern, especially at lower temperatures and at higher chloride concentrations.

The pitting potential will also be a function of alloying content (and therefore the extent of passivity or corrosion resistance) and will increase with both chromium content and molybdenum content; thus nickel-base alloys and ferritic or austenitic stainless steels (and especially molybdenum-containing Type 316 stainless steel) will exhibit better pitting resistance than lower alloyed materials.

(b) Once the conditions for oxide breakdown have been met, then localized corrosion, or pit growth, may occur at a rate that is, amongst other parameters, a function of the degree that the corrosion potential exceeds the pitting potential, and the maintenance of the aggressive environment in the growing pit (i.e., the conditions discussed in the section on crevice chemistry).

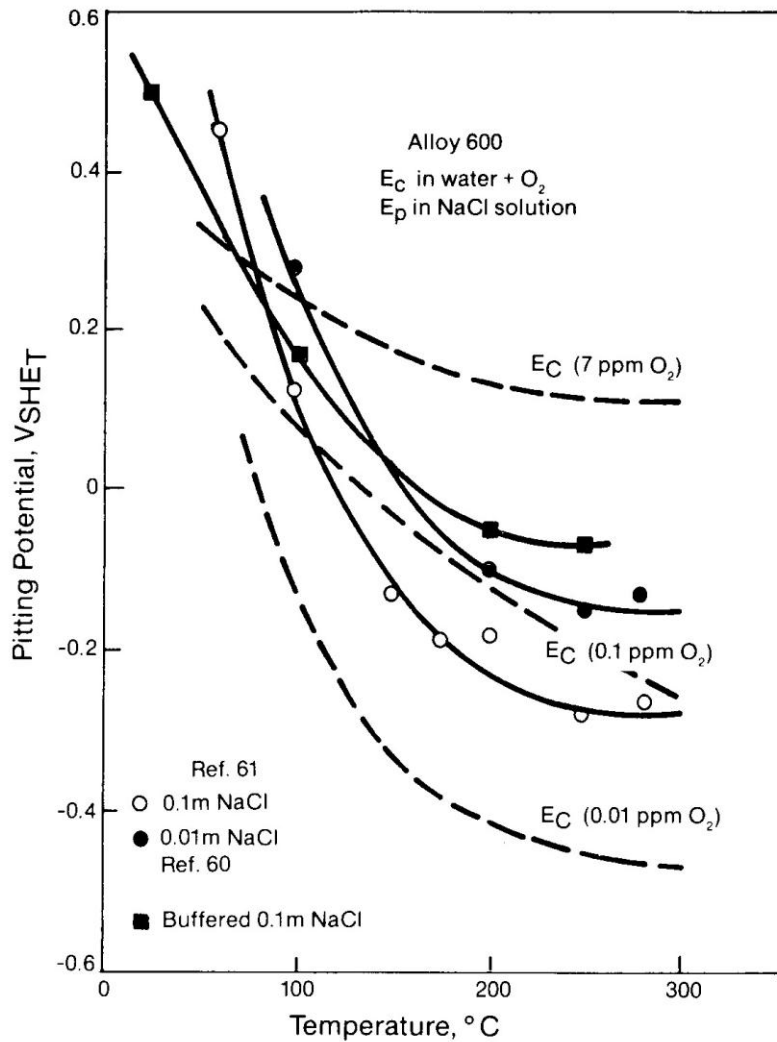


Fig. A.14. Pitting, shown by the solid lines, and corrosion potential, (E_c), shown by the dashed lines, for Alloy 600 in water containing chloride anions as a function of temperature. [26, 27] (© NACE International 1985)

Although the essential controlling parameters of importance in the initiation and growth of pits are known, it is also apparent that many of these parameters are dependent on random events [28, 29] and that, therefore, there will be a distribution associated with both the stochastic [28, 29] and deterministic model [30, 31] predictions. Such effects on the variability in predictions are discussed in separate background papers [see Appendices B.15 and B.19]. Regardless of these aleatory uncertainties, the basic knowledge of the conjoint conditions for pit initiation and growth exists, thereby allowing management of potential pitting damage in LWR systems. This knowledge includes the material choice and degree of environment (water purity, flow rate) control that is needed. Prediction uncertainties arise when there are unanalyzed changes in plant configuration; an example of this might be the removal of certain insulation materials from stainless and carbon steel piping, e.g., mitigation of sump screen blockage concerns, when the chemical makeup of that insulation material (for example, silica) might be conferring pitting (and stress corrosion cracking) resistance to the piping.

Galvanic Corrosion

Galvanic corrosion is the loss of material, generally measured as a **local** rate of loss of surface material, caused when two materials with substantially different corrosion potentials are in electrical contact in the presence of a corrosive (and electrically conductive) environment. In such cases the corrosion rate of the more active material (i.e., that with the more negative corrosion potential) is increased, with the magnitude of that increase being a function of the relative areas of the two metals, and the difference in corrosion potentials. Thus the corrosion rate of mild steel condenser tube sheets exposed to seawater may be increased by a factor of 3-7 in the area adjacent to a copper based condenser tube that is rolled into it, with the precise acceleration factor being a function of the excess area of the copper tubes. Similarly, carbon and low alloy steels in service water environments have substantially lower corrosion potentials than stainless steels and titanium alloys, and would be preferentially attacked in a galvanic couple.

As with general corrosion, galvanic corrosion is a well-understood phenomenon, being the theoretical basis for sacrificial anode protection techniques used in many industries. Consequently, although the possibility of galvanic corrosion exists, it is relatively rare in reactor service since the corrosion potentials of the various materials in the higher temperature systems are reasonably similar, and in the lower temperature systems involving large surface areas in cooling water such as condensers [32] the phenomenon is generally accounted for at the reactor design and construction stage.

Microbiologically Influenced Corrosion (MIC)

MIC is associated with the presence and biological activity of various bacteria and fungi which, upon interaction with nutrients in the environment, produce organic acids that may lower the local pH level to 2.5 thereby increasing the metal corrosion rate (Figure A.1). The "environment" in this case may be not only untreated service water, for example, but also greases applied to external structures for general corrosion protection [33]. Damaging species other than organic acids may be formed which are specific to the bacteria and fungi microorganism [see Appendix B.16]. For instance, anaerobic sulphate-reducing bacteria (SRB) produce reduced sulphur compounds that may increase the localized corrosion rate of carbon and low-alloy steels. On the other hand, aerobic bacteria, which require oxygen for survival, are sulphate oxidizing, producing sulphuric acid, and a local increase in acidity. In addition such bacteria form slimes, which cover the metal surface, thereby creating an oxygen-starved region that allows the development of anaerobic bacteria. In such cases, biological fouling can be so severe that it not only forms corrosive crevices, but can also block flow in service water piping.

These various bacteria each have very specific conditions of survival in terms of pH, temperature, dissolved oxygen content, and supply of appropriate nutrients. From a control viewpoint, however, MIC is not expected for any extended period at temperatures above 99°C or in borated- or hydrazine treated water. For instance, treated water systems, such as PWR borated emergency core cooling systems, have operated for many years with no evidence of MIC. However, damage might be expected in cooling water and service water systems that have a flow rate low enough to ensure an adequate nutrient supply rate without physically removing the bacteria. Another process that exacerbates MIC is the intermittent flushing of water lines that are otherwise stagnant, such as fire protection lines. The periodic flushing introduces new nutrients to the stagnant lines, increasing biological activity and increasing the risk of bacteriologically induced corrosion and fouling. Consequently, MIC damage has been observed in LWR structures such as carbon and stainless steel piping and tanks, copper-nickel, stainless steel,

brass and aluminum bronze cooling water pipes and tubes, especially during construction, hydrotest and outage periods [4]. Effective control in these potentially susceptible systems is achieved by the use of biocides and controlling the nutrient supply rate.

Environmentally Assisted Cracking

Environmentally assisted cracking is closely related to the principles of other localized corrosion phenomena, such as pitting, crevice corrosion and intergranular attack, and these may well act as the precursor [see Appendix B.15] to sustained crack initiation and growth when that localized corrosion process has the added contribution of tensile stress.

Environmentally assisted cracking phenomena cover a wide spectrum of degradation modes, categorized in terms of stress corrosion cracking, hydrogen embrittlement, strain-induced cracking, and corrosion fatigue. Even within these categorizations there are submodes that may be defined in terms of the morphology of cracking (e.g., transgranular, intergranular, interdendritic, granulated), the effect of specific environments (e.g., irradiation, “external, contaminated,” primary-water) or subsets of an existing cracking mechanism (e.g., low-temperature crack propagation as a subset of hydrogen embrittlement). To a large extent such a confusing categorization has arisen because of the historical nature of the first laboratory and reactor observations, plus the fact that, at that time, it was not recognized that many of the cracking modes were not new mechanisms, per se, but merely associated with changes in a rate controlling parameter. For instance, as shown in Figure A.15, the subcritical crack propagation rates in stainless steels strained at various rates in oxygenated water at 288°C have a monotonic relationship with strain rate; those observed at slow strain rates, associated with creep under constant load (e.g., stress corrosion cracking), are an extension of both those observed under applied, monotonically-increasing strains (e.g., strain induced cracking), and those at even higher applied strain rates under cyclic loading (e.g., corrosion fatigue). Thus, for this system, there is no difference in the environmentally enhanced crack propagation mechanism between stress corrosion cracking, strain induced cracking and corrosion fatigue, although the sensitivity of the cracking response to e.g., environmental or material conditions may change significantly at different strain rates. Similarly the effects of irradiation on the cracking susceptibility are now recognized as merely changing the rates of various rate-controlling parameters, rather than introducing an entirely new mechanism of crack propagation.

It has long been recognized that there are three requirements for environmentally assisted cracking to occur (Figure A.16); a “susceptible” material condition, an “aggressive” environment and a tensile stress. The extent of these conjoint criterion will change with the specifics of the system but, in general, if one of these attributes is completely absent then the cracking phenomenon will not occur; this very qualitative observation was the root of many of the early mitigation actions, e.g., stress corrosion cracking in BWRs.

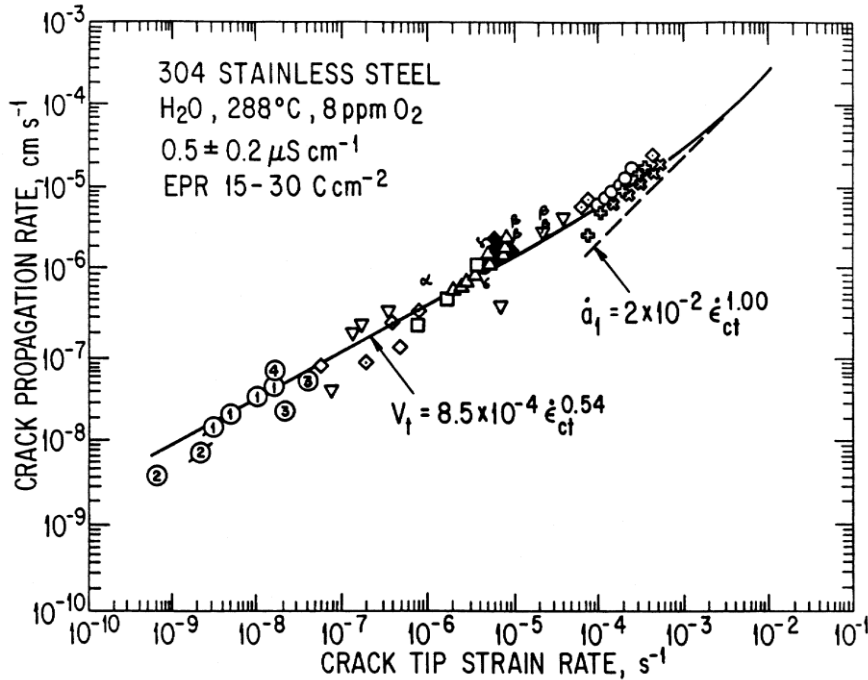


Fig. A.15. Observed and theoretical crack propagation rate vs. crack tip strain rate relationships for sensitized 304 stainless steel in oxygenated water at 288°C. (© NACE International 1990) Note that the numbered data at the lowest crack tip strain rates were obtained under constant load or displacement conditions, whereas the data marked by geometric symbols were obtained under cyclic loading. Intermediate data, identified by Greek symbols where obtained under monotonically rising “slow strain rate” conditions [34, 35]

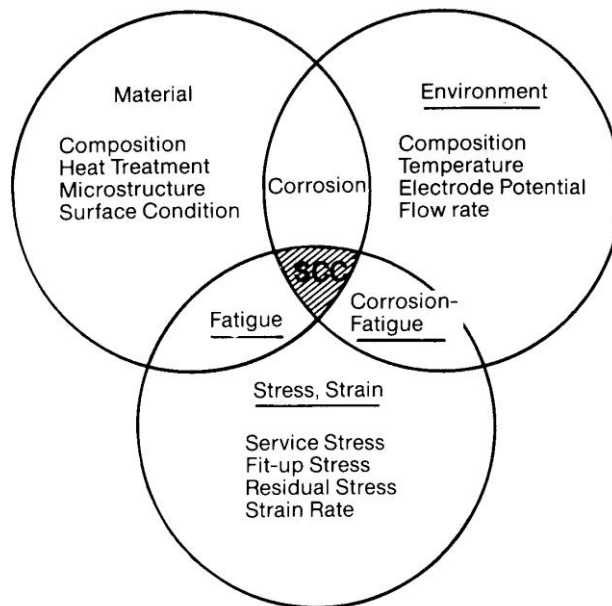


Fig. A.16. Conjoint material, stress and environment requirements for stress corrosion cracking [36] (Courtesy of Plenum Press)

The management of environmentally assisted cracking has moved in the last 25 years beyond reliance on a largely qualitative understanding of the various phenomena inherent in Figure A.16, to the development of a quantitative understanding of the multidimensional interactions between the parameters that control the cracking susceptibility, backed up by an understanding of the mechanisms of crack initiation and propagation. Such developments are central to the definition of appropriate inspection procedures. The fact that the system parameters are not always defined adequately, and the interactions between these parameters are not always well quantified or understood from a mechanistic viewpoint, are the basic reasons why stress corrosion cracking appears as a potential concern area for so many of the reactor systems in Table A.5.

The challenges in predicting the occurrence of environmentally assisted cracking were discussed in Sections 2.5 and 4.2, and several background papers in Appendix B listed below address specific issues associated with, for instance, irradiation, the overall environment, and the alloy composition:

- SCC of Sensitized and Non-Sensitized Austenitic Stainless Steels and Weldments [see Appendix B.1]
- IASCC of Stainless Steels and Other Irradiation Phenomena [see Appendix B.2]
- SCC of Alloys 600, 690, 182, 152 and 52 in PWR Primary Water [see Appendix B.6]
- Corrosion of Steam Generator Tubes [see Appendix B.7]
- Stress Corrosion Cracking of Carbon and Low Alloy Steels [see Appendix B.8]
- Environmental Degradation of High Strength Materials [see Appendix B.9]
- Degradation of Fracture Resistance; Low Temperature Propagation (LTCP) in Nickel-Base Alloys [see Appendix B.13]

In many of these systems there is a considerable database to allow analysis of the effects of system variables on the cracking response. In some cases, however, there is cause for concern about the data quality (due to lack of experimental control during older data collection programs), which gives rise to excessive data variability and, therefore, uncertainty in the predictions of future behavior. In other cases the variability is to be expected due to the stochastic nature of some of the cracking phenomena [see Appendix B.7] and, in such cases, there are well-accepted data analysis techniques [see Appendix B.19] to address this. In other systems (such as stress corrosion cracking of carbon and low alloy steels [see Appendix B.8] and austenitic stainless steels under unirradiated [see Appendix B.1] and irradiated [see Appendix B.2] conditions), there is sufficient mechanistic understanding of the effects of the various system variables to give assurance that the potential cracking in the future could be mitigated. However, in other systems (such as stress corrosion cracking of some nickel base alloys in PWR primary coolant [see Appendix B.6] at operating temperatures, or under dynamic straining conditions at lower temperatures [see Appendix B.13], further development of mechanistic understanding of the cracking process will provide adequate support to data-based mitigation actions.

The following discussion presents a relatively high level treatment of some of these topics in order to provide a background to the details given in the topical reports in Appendix B. Focus is placed on certain aspects of environmentally assisted cracking which are highlighted in the PIRT panel judgments; namely changes in the morphology of cracking (transgranular vs. intergranular), the effect of environment (effects of irradiation and PWR primary water) and “new” modes of cracking (low temperature crack propagation).

Intergranular Stress Corrosion Cracking (IGSCC)

IGSCC is associated particularly with the cracking of austenitic alloys used in, e.g., stainless steel piping (Figure A.17) and internals and in nickel base alloys in BWRs. The specifics of IGSCC of nickel-base alloys in PWR primary environments are discussed in a separate part of this section. Under BWR operating conditions the conjoint requirements for cracking given in Figure A.16 correspond to an environment that is oxidizing (due to an excess of radiolytically-produced oxygen or hydrogen peroxide), a microstructure that is “sensitized” (due to thermal sensitization during welding and/or stress relief heat treatment) to produce a chromium depleted region adjacent to the grain boundary, and a tensile stress associated primarily with weld residual stresses.

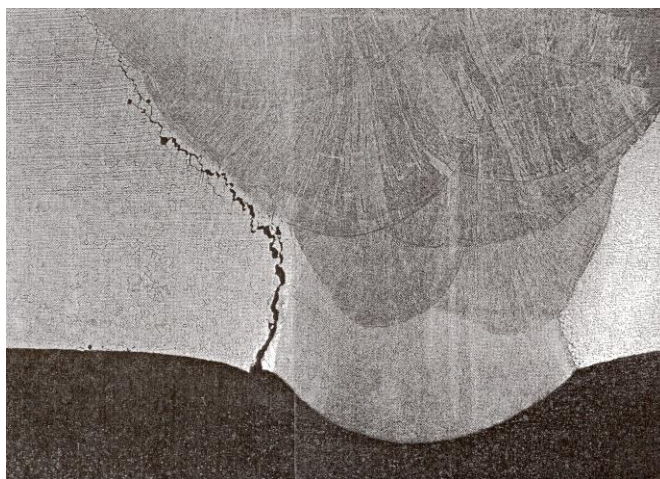


Fig. A.17. IGSCC in a 400 mm (16 in.) diameter welded Type 304 pipe exposed to oxygenated water at 288°C. Note propagation adjacent to the weld heat affected zone, in a region associated with maximum grain boundary chromium depletion and weld residual tensile stress [37]

IGSCC has been extensively researched [34,35,37,38] and is considered, at least for austenitic stainless steels and nickel-base alloys in BWRs, to proceed primarily by a slip oxidation (dissolution) mechanism [34,35], which relates the propagation rate to the continual rupture of the protective oxide at the crack tip and the associated increase in oxidation rate in this region. This process (Figure A.18) has been successfully quantified in terms of key parameters such as crack tip strain rate (i.e., a function of applied/residual stresses), corrosion potential and conductivity (i.e., functions of surface chemistry/bulk water composition) and material composition/microstructure (i.e., function of fabrication conditions).

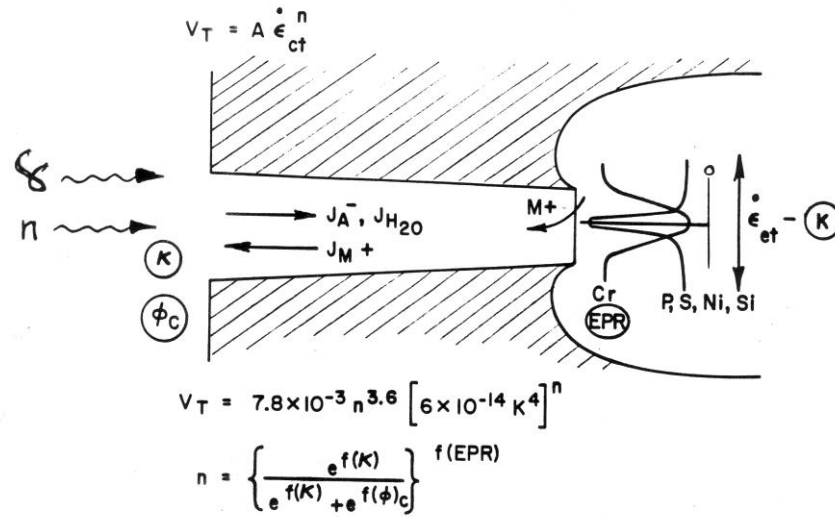


Fig. A.18. Schematic of the crack enclave and the relevant phenomena associated with the slip oxidation mechanism of crack advance. Quantification of these phenomena has led to a life prediction methodology for austenitic stainless steels and nickel-base alloys in BWRs. [34, 35]

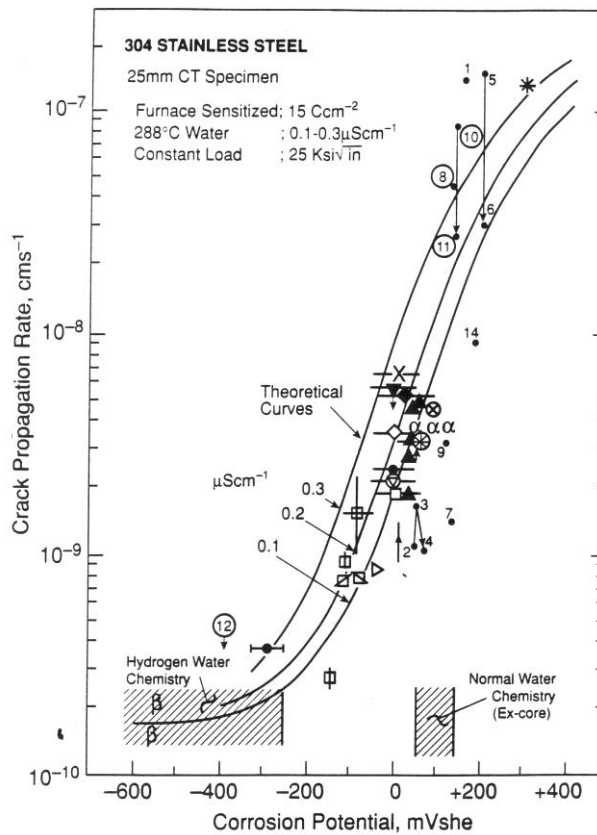


Fig. A.19. Observed and predicted dependency between crack propagation rate for sensitized stainless steel and corrosion potential. [34, 35]

Mitigation of IGSCC is focused primarily on improved coolant chemistry (e.g., hydrogen water chemistry (HWC) and dissolved impurity reduction in BWRs, [see Appendix B.10] sometimes together with surface modification of the component (e.g., Noble Metal Chemical Addition (NMCA) or zirconia coating). For instance the predicted and observed benefit of reducing the corrosion potential of sensitized stainless steel in 288EC water and consequently decreasing the stress corrosion crack propagation rate is apparent in Figure A.19. Such a mechanistic understanding and data base offers the quantitative rationale for adopting HWC and NMCA water chemistry control in BWRs. Such an understanding also explains the generally high stress corrosion resistance of stainless steels in the deaerated PWR secondary circuits where the corrosion potentials are low. Similar rationales are available to support the control of anionic impurities; especially chloride and sulphate (see Appendices B.1 and B.10).

Stress reduction has also been used extensively (e.g., weld overlays for piping and clamps for internals in BWRs, improved tube support plate structures in PWR SGs, etc.). The primary emphasis has been on significantly reducing crack growth since minor intergranular attack (IGA) of austenitic alloys, which is a common initiating precursor, is often present from fabrication, and/or cannot be prevented in operation. As indicated in Figure A.20, the quantitative understanding of the mechanism of crack propagation gives support to data-based estimates of the benefits of various mitigation actions, thereby offering assurance about successful future plant performance.

Key areas for further research include the effects of cold work (including local strain concentration in weld heat-affected zones) and the behavior of cast stainless steels and nickel-based weld metals, as well as the influence of specific, deleterious coolant impurities (e.g., lead, residues from ion exchanger resins). All of these topics are covered in greater detail in appendix B and in Section 3.3 "Generic Materials Degradation and Life Management Issues."

IGSCC of carbon and low alloy steels does not normally occur in LWR media [see Appendix B.8], but limited cracking of this type has been observed in CANDU reactors and it should also be considered a possible degradation mechanism in concentrated boric acid environments, such as might form on external surfaces following leakage of PWR primary coolant.

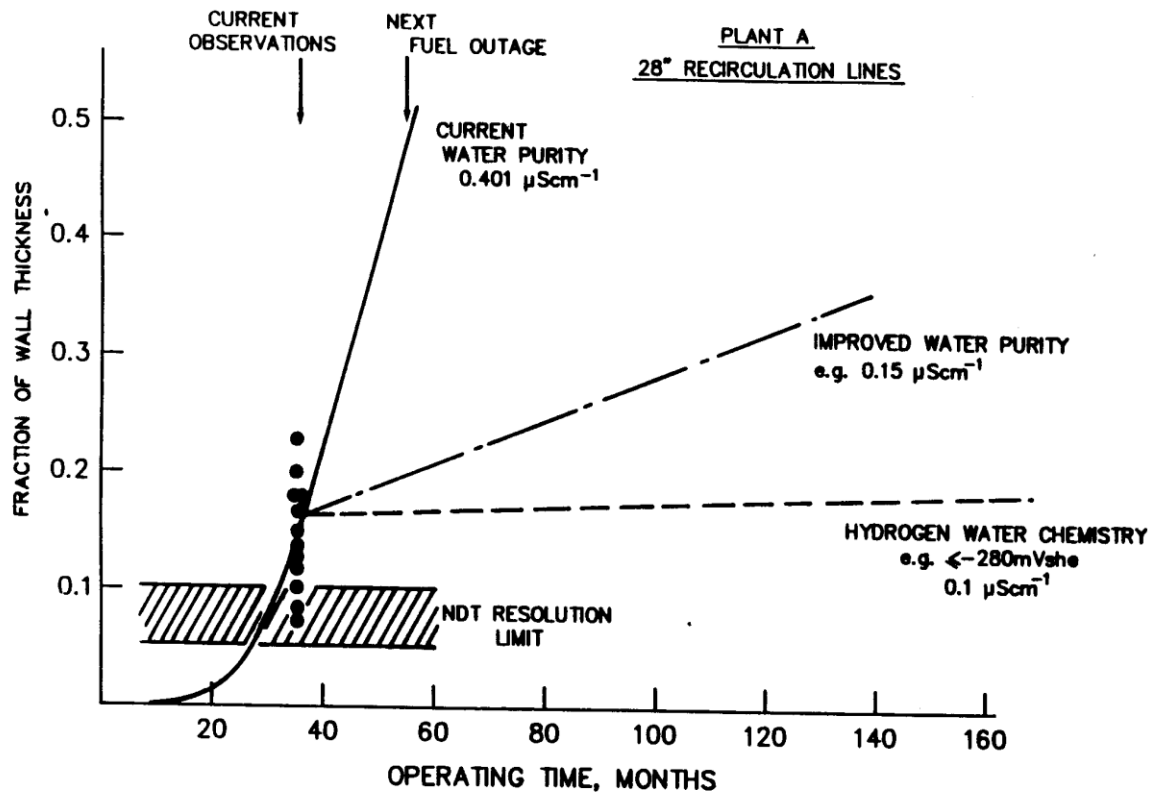


Fig. A.20. Predicted response of defected piping for defined changes in water chemistry in BWR plant. [35] (© NACE International 1990).

Transgranular Stress Corrosion Cracking (TGSCC)

TGSCC may be observed in solution-annealed stainless steels since there is no metallurgical feature in the grain boundary akin to grain boundary chromium depletion in the sensitized condition to concentrate the corrosion processes in that region. In such cases the extent of cracking is governed by slip features that maintain a high oxide rupture rate at the crack tip, and environmental conditions such as the corrosion potential (i.e., function of dissolved oxygen or other oxidants) and aggressive impurities (e.g., chlorides) that affect the chemistry at the crack tip (see earlier discussion on crevice chemistry). As would be expected from the discussion above on IGSCC it is possible to transition from IGSCC to TGSCC morphologies depending on the materials' degree of sensitization, slip characteristics (i.e., function of yield stress or degree of cold work) and dissolved oxygen/chloride content. An example of such transitions is shown in Figure A.21. It is apparent that TGSCC would not be expected to be a common phenomenon under normal BWR and PWR water chemistry regimes. However, as pointed out in the main report, such TGSCC incidences may become of importance for stainless steels, especially if the surface is highly cold worked, or on external component surfaces which may be contaminated with chloride deposits, or, in dead legs (e.g., for CRDMs and canopy seals in PWRs.) where impurities cannot be dispersed.

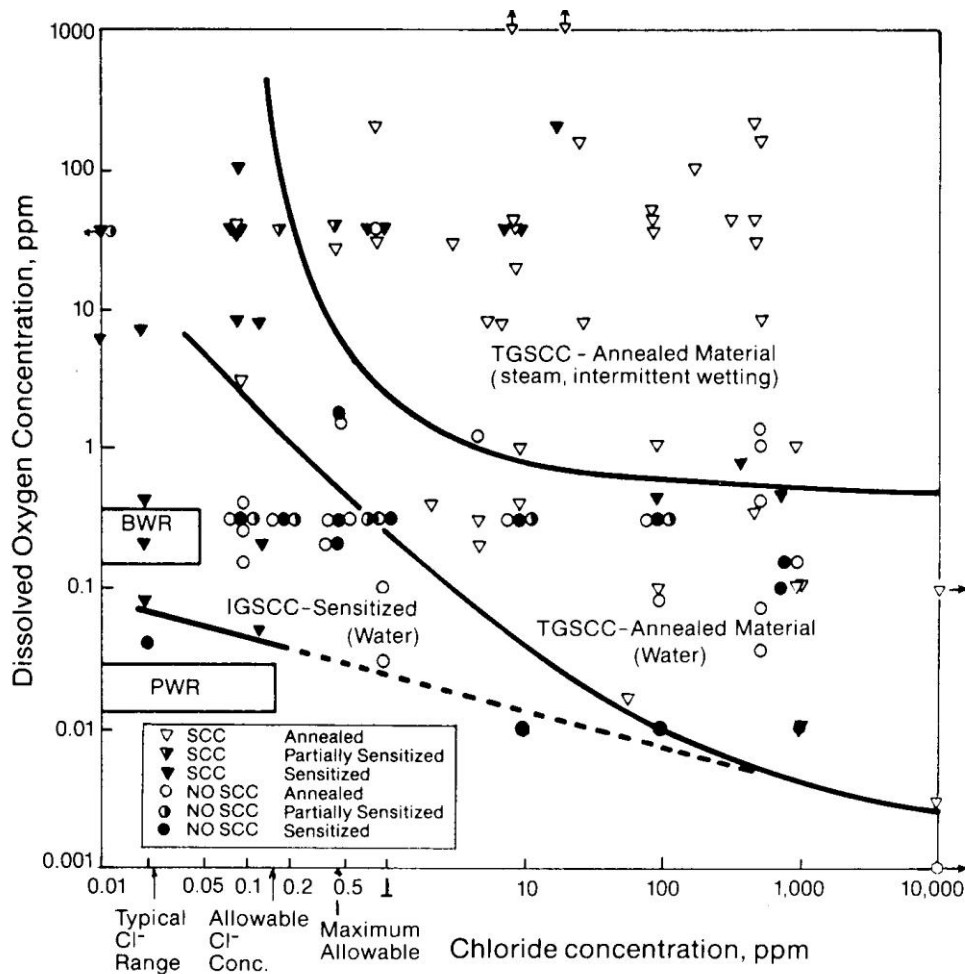


Fig. A.21. Effect of oxygen and chloride concentration on the SCC of austenitic stainless steels in 250-350°C water, together with the oxygen/chloride ranges in BWR and PWR environments. [38] (© NACE International 1980)

As discussed in Appendix B-8, although the ferritic carbon and low alloy steels are regarded as resistant to SCC under well controlled LWR operating conditions [see Appendix B.6], limited TGSCC has been observed, e.g., in SG shells exposed to faulted secondary water, and in BWR components subjected to high, local loads while operating with normal (oxygenated) water chemistry. Recent research suggests that occasional susceptibility may also be related to chloride chemical transients and changes in the deformation behavior of particular low alloy steels associated with the dynamic strain aging which can occur at intermediate operating temperatures.

Primary Water Stress Corrosion Cracking (PWSCC)

PWSCC refers to intergranular cracking of any material, but particularly of Ni- base alloys such as Alloy 600 and its weld metals, Alloys 182 and 82, in PWR primary coolant (i.e., containing lithium, boric acid, and hydrogen). Figure A.22 illustrates the main locations where PWSCC has occurred [see Appendix B.6], whereas the schematic drawing in Figure A.23 illustrates the relationship between the shape of the axial crack in the Alloy 82/182 weld and Alloy 182 butter and the dissimilar metal low-alloy steel and stainless steel components.

Alloy 600/82/182 Locations

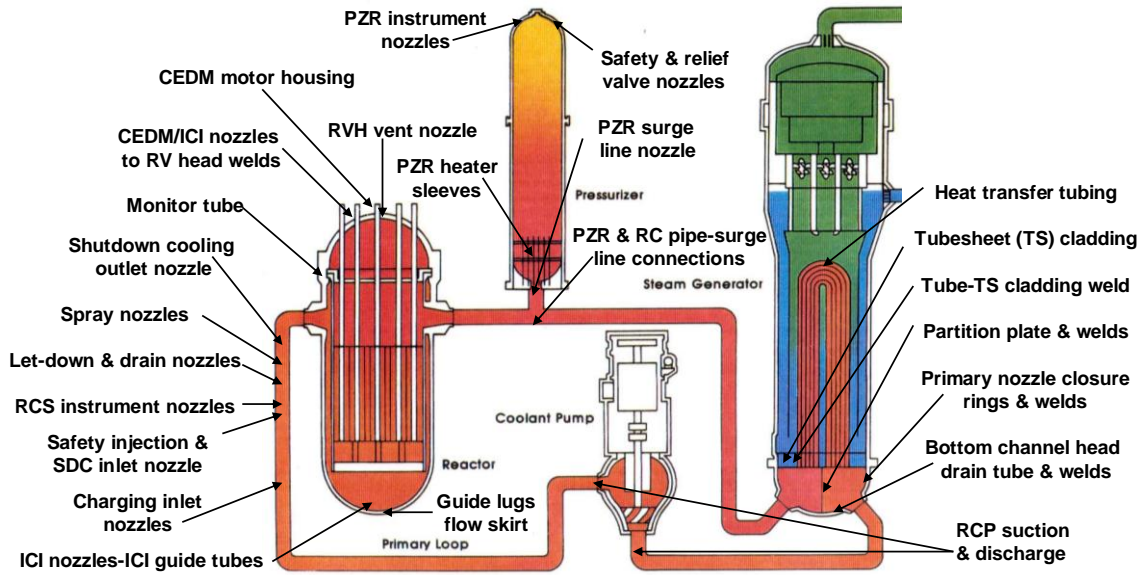


Fig. A.22. Regions in the PWR Primary Reactor Coolant System where PWSCC of nickel base alloys have been observed.

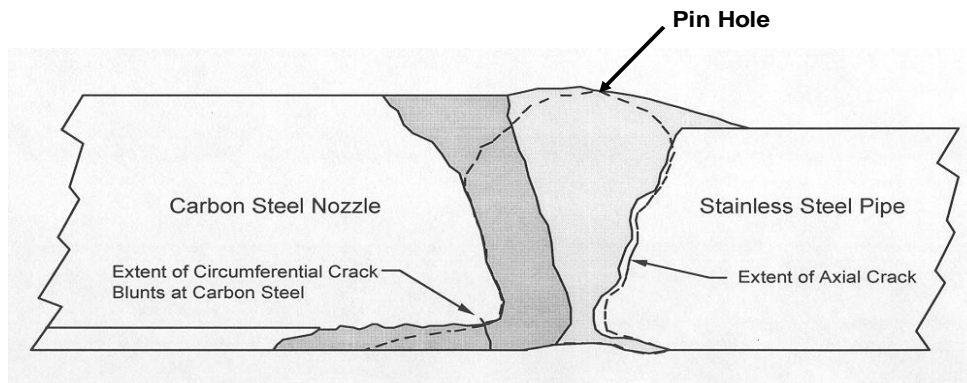


Fig. A.23. Schematic diagram illustrating the locus of an axial PWSCC crack front in the Alloy 82/182 weld between dissimilar alloy carbon and stainless steel components.

Over the last thirty years, intergranular stress corrosion cracking in PWR primary water (PWSCC) has been observed in numerous components made of these nickel-base alloys sometimes after relatively long incubation times. In stark contrast to IGSCC of Ni-base alloys in other media (e.g., on the PWR secondary side) or austenitic alloys in BWRs discussed above, sensitization of the material through intergranular precipitation of chromium-containing carbides is beneficial to the PWSCC resistance of Alloy 600, which justifies its consideration in a separate category of cracking mechanism. However, large variations exist in the susceptibility of individual heats of material, even of nominally similar composition and thermomechanical processing history, so that prediction of service behavior is difficult. Cold work is highly detrimental, in agreement with observations in many other stress corrosion alloy/environment systems in LWRs.

Cracking, which can also occur in pure hydrogenated water or steam, is highly temperature-dependent and is associated with environmental conditions under which the surface films are in the transition region of Ni/NiO stability. Despite intensive research, there is no general agreement on the mechanism of PWSCC. Candidate theories include hydrogen assisted cracking, slip oxidation, thermally activated dislocation creep and internal oxidation. The latter has a particular attraction, since it could explain the very long times (>100,000 hours) sometimes necessary for cracking to initiate, even under conditions where subsequent crack propagation is relatively rapid. PWSCC of weld metals (and its possible interaction with fabrication defects such as hot cracking) is currently a high-profile topic that has been insufficiently studied and is not well understood.

To date, mitigation of PWSCC has usually involved repair and replacement actions using more resistant materials (such as Alloy 690). In addition, increased attention is now being paid to possible mitigation measures involving surface treatment (e.g., water-jet peening), chemistry optimization (e.g., adjustment of hydrogen levels and/or addition of potentially inhibiting species such as zinc), and various mechanical options to achieve a reduction in tensile stress levels.

Irradiation Assisted Stress Corrosion Cracking (IASCC)

The SCC behavior of irradiated stainless steels is a natural extension of IGSCC of un-irradiated stainless steel [see Appendix B.2], but the critical fluence level above which irradiation effects begin to dominate material behavior is hard to define because of the interactions of several material, stress and environmental factors. A lower value of $\sim 5 \times 10^{20}$ n/cm² is often quoted for BWR internals, with saturation of the irradiation effects beginning at around 3×10^{21} n/cm², i.e., shortly before the expected end-of-life (EOL) fluence of $\sim 8 \times 10^{21}$ n/cm². In contrast, IASCC in the very different primary water chemistry in PWRs has only been observed (e.g., in baffle/former bolts) to start after reaching a fluence of $\sim 2 \times 10^{21}$ n/cm² and little information is available about expected behavior near the much higher EOL fluence values typical of PWRs.

The mechanism of IASCC in PWR primary water is currently unclear, with no evidence that locally oxidizing conditions, grain boundary segregation, helium formation, or hydrogen embrittlement play a major role, although high strength from irradiation hardening does appear to be important (possibly analogous to the effects of cold work in SCC without irradiation). Mitigation measures are not yet available.

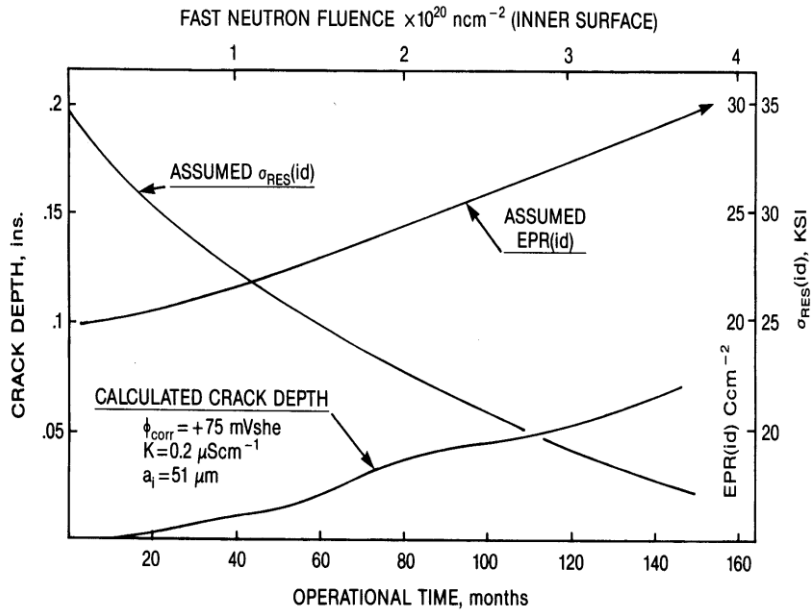


Fig. A.24. Calculated change in crack depth in irradiated stainless steel as a function of fluence (e.g., time) due to specified changes in residual stress and degree of grain boundary sensitization. [see Appendix B.2]

By contrast, the mechanistic understanding of the roles that irradiation has on stress corrosion cracking of stainless steel core components in BWRs, and its relationship to the cracking that occurs in thermally sensitized microstructures, is relatively advanced [see Appendix B.2] and this has an impact on the judgments of the future IGSCC/IASCC performance of such components. For instance, apart from its role in reducing fracture toughness, irradiation in BWRs is best viewed as an accelerant of many of the features shown schematically in Figure A.19. For instance, fast neutron irradiation increases the extent of grain boundary chromium depletion, it affects the crack tip strain rate through both irradiation induced hardening and relaxation of the residual stresses and, finally there is an elevation of corrosion potential. Such interacting irradiation effects affect the IASCC cracking kinetics in a sometimes non-monotonic fashion, as illustrated in Figure A.24.

Mitigation of IASCC in BWRs is focused primarily on reductions in corrosion potential through the use of HWC/NMCA, and the improvement in water purity, i.e., an extension of the approaches already taken for IGSCC.

Low-temperature Crack Propagation (LTCP)

LTCP refers both to high sub-critical crack growth rates (i.e., SCC, most likely from hydrogen assisted cracking) and to reduced fracture toughness [see Appendix B.13]. Such degradation has been observed in laboratory tests on nickel-base alloys under very specific conditions of temperature, strain rate and the extent of hydrogenation, and is of potential concern in PWR primary systems operating under very limited conditions. While the greatest concerns are for higher strength Ni alloys (e.g., Alloy X750 and Alloy 182/82 weld metals), there are possible concerns for base metals (such as Alloy 600 or 690), particularly (but not only) if the yield strength is elevated (e.g., from cold work or irradiation).

Initial studies in the 1980s [39, 40] showed very rapid crack propagation in the temperature range 70-140(C in moderate to high strength Ni base alloys once IG SCC cracks had formed in high temperature water. The highest rates were observed in Alloy X750, although large effects were also observed for Alloy 182 and 82 weld metals and other Ni base alloys (e.g., aged Alloy 625, Alloy 718, and Alloy 690). The observations occurred in constant displacement (wedge/bolt loaded) specimens, in actively loaded specimens, and also in specimens exposed only to gaseous hydrogen in this temperature regime (leading to the reasonable conclusion that it's a hydrogen related phenomenon). . More recently, it has been observed that significant reduction in fracture toughness (e.g., in J-R tests) can occur in the same temperature regime, under very specific loading rates.

The fact that these degradation effects are only observed when the specimens have been exposed to hydrogen (e.g., hydrogenated water) above a specific level strongly implies that the mechanism of both embrittlement and increased subcritical crack propagation is related to hydrogen embrittlement. However, the exact mechanism is unknown, and the conjunction between the PWR plant operations and the observed requirements of temperature, alloy content and microstructure, and strain rate for these degradation phenomena to become significant, is the object of high priority studies.

A.4.3 Under-clad Cracking and Clad Disbonding

Three types of cracking have been recognized as potentially affecting the heat affected zones of bimetallic joints such as those made between low alloy reactor pressure vessel steels and overlay cladding of austenitic stainless steel: hot cracking (sometimes called liquation cracking), reheat cracking and cold cracking.

Hot cracking usually arises from a combination of the formation of a liquid metal phase at grain or dendrite boundaries at very high temperatures during welding and the contraction forces that develop during cooling of the weld pool. Due to the high temperature necessary for such cracking, it is only encountered in the deposited weld metal or very close to the fusion line. Under-clad cracks of this type are therefore <1 mm in depth below the cladding. They are rarely found when cladding low alloy steel and do not lead to clad disbonding.

Reheat cracking [41] occurs as a result of a creep mechanism during stress relief heat treatments at temperatures in excess of 550°C. In practice, the low alloy pressure vessel steels used in the nuclear industry are relatively insensitive to this form of cracking except in zones of elemental segregation (C, Mn, Mo, S, and P). When observed, the cracks are perpendicular to the fusion line, less than 4 mm in height, and are situated exclusively in zones of large grains that may be formed in the heat affected zone where two successive weld beads overlap. The large grain zones have reduced ductility that allows intergranular cracking to develop under the influence of the stresses arising from the difference in coefficients of thermal expansion of austenitic and ferritic steels. Creep cavities are easily seen on the intergranular facets generated by reheat cracking. This cracking phenomenon is avoided by adjusting the welding procedures to avoid the development of large grain heat affected zones.

Cold cracking [42-44] is caused by the combined action of residual welding stress and hydrogen introduced into the substrate low alloy steel during welding. Three factors are associated with the appearance of this cracking: a mixed martensitic-bainitic microstructure in the heat affected zone of the low alloy steel; residual welding stress (that typically reaches a maximum 5 to 10 mm from the fusion line); high concentrations of hydrogen in the low alloy steel heat affected zone after welding (with up to 15 ppm in the austenitic weld deposit) compared to <0.2 ppm in

the base material before welding. The hydrogen originates from moisture absorbed by the coating of weld electrodes or by the flux used for strip cladding. Hydrogen diffuses into the substrate low alloy steel heat affected zone where it may reach temporarily 10 ppm while the temperature is high enough for the metal to be austenitic. The susceptibility of the heat affected zone is enhanced by the presence of zones of elemental segregation (C, Mn, Mo, S, P), particularly in large forgings. The cracks have a mixed intergranular and transgranular quasi-cleavage morphology. Usually, due to constraint, the cracks are orientated perpendicular to the fusion line with defect heights typically up to 7 mm, exceptionally up to 12 mm. In some special cases, (e.g., welding on a re-entrant angle, which leads to stresses perpendicular to the interface, and in the presence of a hard zone with precipitates at the fusion boundary), cracking may take place parallel to the fusion line and lead to clad disbonding. The main remedies are to ensure adequate preheat, interpass and post weld soak temperatures that allow the hydrogen to diffuse away prior to stress relief, to keep welding consumables as dry as possible, and to avoid as much as possible weld cladding the most segregated zones of low alloy steel forgings.

A.4.4 Fatigue

This section addresses materials degradation due to fatigue, an aging degradation mechanism that can affect a number of major components throughout the primary pressure boundary of both PWRs and BWRs. [see Appendix B.14]. Components that may be affected range from the low alloy steel reactor pressure vessel, pressurizer, and steam generator shell to stainless steel pumps, piping etc. to nickel base alloy welds, tubing, etc. This degradation mode is an extremely well researched topic, fatigue being, unlike many of the other degradation modes, considered in the original reactor design basis.

From a categorization viewpoint, fatigue may be regarded in terms of “High Cycle Fatigue,” “Low Cycle Fatigue,” “Thermal Fatigue” and “Environmental (or Corrosion) Fatigue.” Superimposed upon these categorizations is the (sometimes semantic) division of degradation periods between “initiation” and “propagation.” Some of these categorizations and environmental impacts may be understood in relationship to Figures A.25 (a) and (b). At the reactor design stage the fatigue life, which forms part of the design basis, is calculated from a stress-amplitude vs. fatigue cycle database that relates to the curves in Figures A.25a and A.25b marked “air.” These curves (in this example for carbon steel) are based on data obtained in air at 25°C for smooth cylindrical specimens, fully reversed cyclically loaded under strain control; “initiation” in this case is defined as a drop in maximum load by 25%, which physically corresponds to a crack of 2-3 mm depth.

The categorization of “high-cycle fatigue” refers to a high number of cycles at a relatively low stress amplitude (typically below the material’s yield strength but above the fatigue endurance limit of the material), with the driving force for the cyclic loading coming from, for instance, flow induced vibrations and/or instabilities in thermal mixing of the coolant. On the other hand “low-cycle fatigue” refers to the higher stress/strain amplitude regime, where the local yield stress may be exceeded leading to correspondingly shorter fatigue lives; such a regime is associated with, for instance, lower frequency operational transients (such as plant start-up/shut-down or hot stand-by). “Thermal fatigue” is due to cyclic stresses/strains that result due to changing temperature conditions in a component or in the piping attached to the component. Thermal fatigue may involve a relatively low number of cycles at a higher stress (e.g., plant operational cycles or injection of cold water into a hot nozzle) or due to a high number of cycles at low stress amplitude (e.g., local leakage effects or cyclic thermal stratification).

Design against fatigue damage is based primarily on the fatigue curves in Section III, Appendix I of the ASME Code. In this design process, the fatigue cycles are decreased from those denoted by the “air” data lines in Figure A.25, in order to take into account the unknown (at that time) effects of a) materials variability and data scatter, b) component size, and c) surface roughness. The extent of this decrease was based on engineering judgment and, as indicated in Figure A.25b, the “design curve” is displaced from the data curve by a factor of two (on stress/strain amplitude) or 20 (on fatigue cycles), whichever was the more conservative. It is this design curve that the fatigue “Cumulative Usage Factors” (CUF) are calculated during the design process aimed at maintaining CUF below 1 through the design life of the component. As discussed in Appendix B.14, there is much discussion internationally about the appropriateness of this “2 and 20” design line, especially when environmental effects need to be accounted for [45-50].

This concern for the effect of the environment on crack initiation is discussed in Appendix B.14, but the essence is illustrated in Figure A.25 for the specific case of carbon steel in LWR environments. It has been demonstrated in several studies that the decrease in the fatigue life below that observed in dry air is a function of the strain rate applied during the loading period, corrosion potential, temperature, and water purity. To a large extent these dependencies are predictable via the knowledge of the environmentally assisted cracking mechanisms discussed earlier [45]. Moreover similar dependencies are observed for most of the ferritic and austenitic alloys in LWRs and as indicated in Figure A.25 (b) for carbon steel piping there are combinations of these system parameters that lead to fatigue lives that are less than the currently accepted design values.

As also discussed in Appendix B.14, there are similar concerns about the effect of the environment on the fatigue crack propagation rates that are used for crack disposition decisions according to ASME XI procedures. In this case significant progress has been made, for the specific case of LAS in PWR reactor water through the introduction of Code Case N-643 [51], which is currently undergoing further refinement.

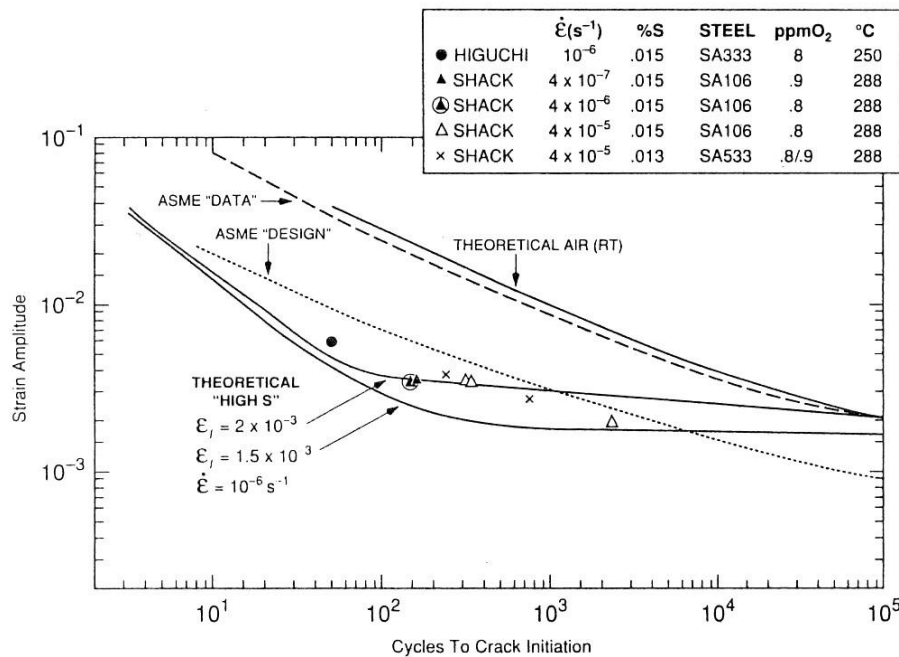
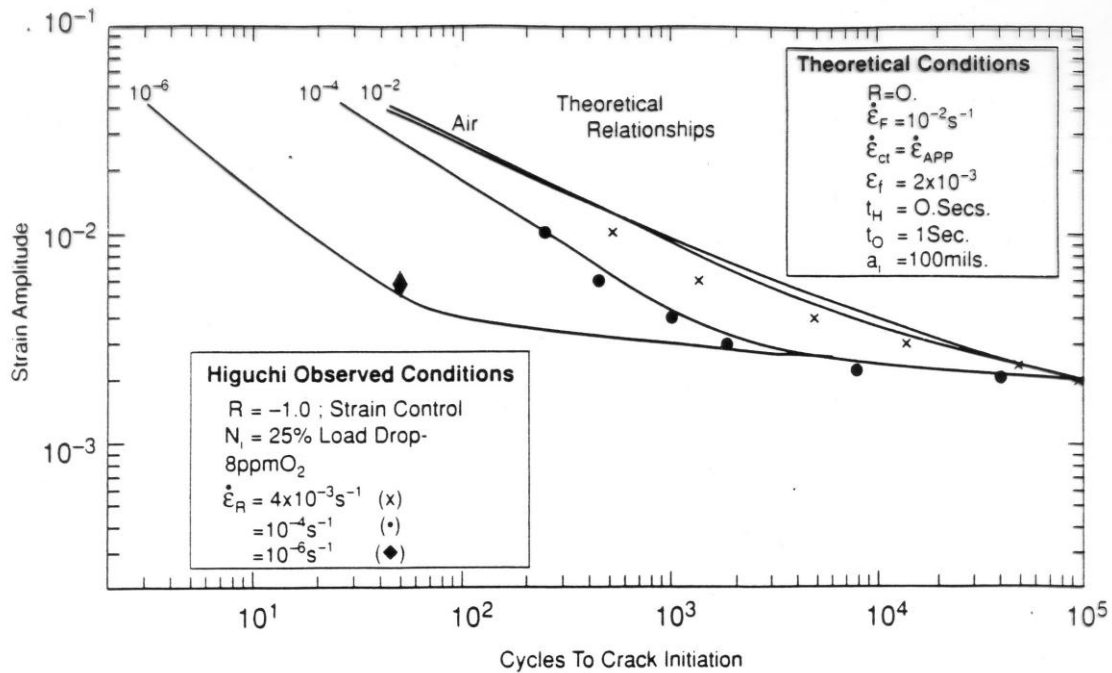


Fig. A.25. (a) Predicted [45] and observed [46] strain amplitude versus cycles to crack initiation relationships for unnotched carbon steel in 288EC, 8 ppm oxygenated water with strain applied at different rates. (b) Predicted [45] and observed [46,47] strain amplitude versus cycles to crack initiation relationships for unnotched carbon and low alloy steels in 288EC water, under the worst combination of material and environmental conditions. (Reprinted with Permission from TMS) Note the non-conservatism of the ASME III design curve under these conditions at certain strain amplitudes

A.4.5 Loss of Fracture Resistance

This section addresses material degradation mechanisms that lead to a reduction in the fracture toughness of the material with increasing time. Because a high level of fracture toughness is a design assumption for the LWR pressure boundary and internal components, degradation mechanisms that lead to reductions of toughness are of high significance.

Two distinct degradation mechanisms, which are relevant to many of the materials of LWR construction, are addressed in this section, radiation embrittlement and thermal aging. In some cases, arguments have been made for synergistic effects between the two degradation modes. An example of this, identified by the NRC in Safety Evaluation Reports, would be cast austenitic alloys in PWRs. To date, however, no data have been presented to prove or disprove the existence of such synergistic effects.

A third loss of fracture resistance issue, associated with some nickel-base alloys after having been exposed to hydrogenated water, and tested at specific loading rates in a specific temperature range was discussed previously in this Appendix, and this is discussed in more detail in Appendix B.13.

Irradiation Effects

- Neutron Embrittlement

Radiation embrittlement results in an increase in the material's yield and ultimate strengths, with a corresponding decrease in material ductility and resistance to flaw propagation (fracture toughness). Radiation embrittlement in ferritic steels is measured by an increase in the ductile-to-brittle transition temperature (RT_{NDT}) and a drop in the Charpy upper shelf energy. Embrittlement in ferritic steels is primarily caused by the formation of copper-rich precipitates that harden the matrix and reduce toughness. Neutron irradiation enhances the formation of these precipitates.

Extensive databases exist for evaluating and predicting embrittlement in reactor vessel steels. These data are obtained from vessel material surveillance capsules in both PWR and BWR vessels, and from test reactors. Embrittlement trend curve models given in various literature citations such as Regulatory Guide 1.99, Rev. 2 are used to predict the shift in RT_{NDT} and drop in upper shelf energy as a function of copper, nickel, and fluence.

Significant variations in radiation embrittlement have also been observed between different types of steel (carbon and low alloy steels, etc.) and even between different heats of the same steel. These differences are caused by variations in metallurgical structure and composition. Improved empirical trend models have recently been developed to describe the combined effects of copper, nickel, phosphorus, irradiation temperature, and neutron flux and fluence on the embrittlement of pressure vessel steels. Steels with a very low copper content show little embrittlement in spite of high radiation doses. The effect of irradiation exposure at low temperatures (below 525°F) increases the rate of embrittlement damage. Weld metal is generally more sensitive to radiation embrittlement than base metal. Impurity chemistry, chemistry variability, and different micro-structure are responsible for the greater sensitivity of the weld metal. In 2002, this improved trend curve model was approved in a revision to ASTM Standard Guide E900.

Stainless steels are also affected by irradiation exposure [see Appendix B.2], but do not exhibit

a ductile-to-brittle transition. In stainless steels, reduction in the ductile fracture toughness properties is associated with microstructural changes resulting from the effects of neutron/atom interactions. Neutrons interact with atoms in the crystal lattice, both directly and indirectly, to displace atoms in the lattice and alter material properties through formation of dislocations, interstitials, and vacancies. Segregation of material impurities also occurs.

Data are available from austenitic stainless steel components exposed to neutron irradiation in experimental and thermal reactors. They show that significant reductions in material J-integral values and tearing modulus values appear at approximately one displacement per atom (dpa). Reductions in these fracture toughness properties appear to saturate at fast neutron exposures greater than 10 dpa.

Currently, there is a lack of substantive fracture toughness data for austenitic stainless steels exposed to a neutron fluence exceeding $\sim 10^{21}$ n/cm² in an LWR environment. The bulk of existing data are developed from materials irradiated in experimental reactors. Differences in neutron spectra of experimental reactors and light water reactors could result in actual material property changes. Specific data regarding irradiation exposure of cast stainless steels in an LWR environment are particularly limited.

- Void Swelling Effects

Void formation is a mechanism in which radiation-induced vacancies accumulate in metal to form microscopic voids. If a large number of voids form, termed void swelling, dimensional changes can occur and loads at connection points (for example, at bolted or welded joints of structural members) may also be altered. Thus void swelling could potentially affect the intended functionality of certain component(s). Based on available fast-reactor data, significant fracture toughness reduction of stainless steels can also occur if void swelling is large (i.e., greater than several percent).

Thermal Aging

Thermal aging [see Appendix B-4] of the duplex austenite/ferrite structures of cast austenitic stainless steels (CASS) has been shown to cause precipitation of additional phases in the ferrite such as formation of a α phase by spinoidal decomposition, nucleation and growth of a α phase, or nucleation and growth of carbides at the ferrite/austenite phase boundaries. Development of these additional phases results in an increase in hardness and yield strength of the casting, with a corresponding reduction in fracture toughness properties. As a result, the component becomes more susceptible to brittle fracture when sufficient tensile loadings are present to drive crack growth. A brittle fracture occurs when the ferrite phase becomes continuous or the ferrite/austenite phase boundary provides an easy path for crack propagation in the presence of an existing flaw and sufficient stresses. This type of failure is due to cleavage of the ferrite or separation of the ferrite/austenite boundary and is termed "channel fracture."

The effects of thermal aging on casting fracture toughness have been shown to saturate once conditions leading to predominantly brittle fracture occur. This saturation effect is associated with development of channel fracture conditions. While the extent of reductions in casting fracture toughness due to thermal aging is related to operating temperature, time at temperature, casting method (static vs. centrifugal), and material composition (molybdenum and ferrite content), available research results indicate that the saturation fracture toughness (C_{vsat}) can be correlated to casting chemical composition, material properties and the casting method. The actual casting toughness decreases logarithmically with increased operating time toward this "infinite-time" saturation value; thus the use of C_{vsat} as a measure of casting fracture toughness is conservative.

Thermal aging embrittlement of materials other than CASS used in reactor components includes (1) temper embrittlement and (2) strain aging embrittlement. Ferritic and low alloy steels are subject to both of these degradation mechanisms but wrought stainless steels are not affected by either mechanism.

Temper embrittlement of low alloy steels is caused by the diffusion and segregation of impurity elements, such as phosphorous, tin, antimony and arsenic, into the grain boundaries after prolonged exposure to temperatures in the range 350°C (662°F) to 575°C (1067°F). At temperatures above this range, the impurities tend toward solution in the ferrite matrix. For example, little or no grain boundary segregation is observed at temperatures above 625°C (1157°F). At temperatures below this range, very long exposure times are necessary for the impurities to diffuse to, and segregate in, the grain boundaries. The presence of carbon tends to accelerate the embrittlement process, due to preferential segregation of the impurities at the interface between grain boundary carbides and ferrite grains. The role of other alloying elements, such as chromium, nickel, magnesium, and molybdenum, in the acceleration or retardation of the temper embrittlement process has been studied extensively. The principal manifestation of temper embrittlement in low alloy steels is an increase in ductile-to-brittle transition temperature, due to the change from predominantly cleavage fracture (before temper embrittlement) to predominantly intergranular fracture along impurity segregation paths (after temper embrittlement).

Strain aging embrittlement occurs in cold worked ferritic steels when they are subjected to temperatures in the range of 260-371°C (500-700°F), and is caused by the pinning of dislocations by interstitial impurities (nitrogen, carbon, etc.). Post-weld heat treatment of reactor vessel components following cold working during fabrication mitigates, but does not eliminate, the effects of strain aging embrittlement. However, following post-weld heat treatment, residual strain aging embrittlement has only a slight effect on the ductility and fracture toughness of LWR vessel component materials under the environmental and loading conditions of interest.